

# Switching Kr/Xe Selectivity with Temperature in a Metal–Organic Framework

Carlos A. Fernandez, Jian Liu, Praveen K. Thallapally,\* and Denis M. Strachan

Energy and Environment Directorate, Pacific Northwest National Laboratory, P.O. Box 999, Richland, Washington 99352, United States

**S** Supporting Information

**ABSTRACT:** Krypton (Kr) and xenon (Xe) adsorption on two partially fluorinated metal–organic frameworks (FMOFCu and FMOFZn) with different cavity size and topologies are reported. FMOFCu shows an inversion in sorption selectivity toward Kr at temperatures below 0 °C while FMOFZn does not. The 1D microtubes packed along the (101) direction connected through small bottleneck windows in FMOFCu appear to be the reason for this peculiar behavior. The FMOFCu shows an estimated Kr/Xe selectivity of 36 at 0.1 bar and 203 K.

Separation of xenon (Xe) and krypton (Kr) is an important problem for industries. Xe has several industrial uses including commercial lighting, imaging, anesthesia, propellant in ion propulsion engines, and so on. Similarly, separating Kr from Xe is an important step in removing radioactive  $^{85}\text{Kr}$  during treatment of spent nuclear fuel.<sup>1</sup> The conventional method to separate these two gases is fractional distillation at cryogenic temperatures, which is an energy intensive process. In addition, even after cryogenic distillation, trace levels of radioactive Kr in the Xe-rich phase are too high to permit further use.<sup>1</sup> If adsorbents could reduce  $^{85}\text{Kr}$  concentrations in the Xe-rich phase to permissible levels, there could be an entirely new supply source of Xe for industrial use.

There are several examples in the literature in which zeolites have been tested for Xe and Kr separation.<sup>1,2</sup> Previous research has shown NaA and NaX zeolite to be selective adsorbents for Xe over Kr with selectivities of approximately four to six.<sup>1,2</sup> Different from zeolites, metal–organic frameworks (MOFs) represent a new class of functional materials consisting of metal centers linked with organic building blocks to produce diverse and customizable structural frameworks.<sup>3</sup> These materials received considerable attention over the past few years because of their high structural stability,<sup>4</sup> high surface areas,<sup>5</sup> large and structurally flexible pore structures,<sup>6</sup> and adjustable chemical functionalities.<sup>7</sup> One key property of these porous materials is the pore size, shape, and structure of MOFs can often be modified to enhance sorbate–sorbent interactions.<sup>8</sup> Although research to date is somewhat limited with regard to noble gases, storage and separation of noble gases have been demonstrated with some MOFs.<sup>9</sup> Our group recently studied two MOFs, MOF-5 and NiDOBDC (DOBDC = 2,5-dihydroxyterephthalic acid), for the facile capture and separation of Xe showing that NiDOBDC adsorbs significantly more Xe than MOF-5 and is more selective for Xe over Kr than activated charcoal.<sup>10</sup> Mueller

et al. reported adsorption of Xe, Kr, and other lighter rare gases using IRMOF-1, which shows this MOF exhibits preferential adsorption of Xe over the rare gases.<sup>9</sup> Another study by the same group found that Cu-MOF has twice the Xe capacity of a high surface area carbon (Ceca, AC-40, 2000 m<sup>2</sup>/g).<sup>9</sup> Snurr et al.<sup>11</sup> and Greathouse et al.<sup>12</sup> simulated the Xe and Kr separation by various MOFs with different topologies and pore sizes using Grand Canonical Monte Carlo (GCMC) simulations. According to Snurr and co-workers the best MOF should have uniform pores that are slightly bigger than the kinetic diameter of Xe for preferential separation of Xe over Kr.<sup>11</sup> Nevertheless, there is no literature available where MOFs can selectively adsorb Kr over Xe. This could be because most MOFs have cavity sizes similar or larger than either of these two gases. Therefore, Xe, a more polarizable molecule, forms stronger van der Waals interactions with the open metal centers inside the MOF pockets, preventing Kr from adsorbing.

Herein, we report Xe and Kr adsorption in two partially fluorinated MOFs (FMOFZn and FMOFCu) showing temperature-dependent selectivities. Particularly, at <0 °C, the FMOFCu shows higher molar selectivity toward Kr based on pure gas isotherms and breakthrough experiments. This is a significant breakthrough because, for the first time, a MOF can be potentially used to selectively remove Kr from Xe mixtures.

Synthesis of FMOFZn and FMOFCu was performed based on the literature procedure.<sup>13,14</sup> The structural analysis of FMOFZn suggest a flexible V-shaped organic building block is connected to two zinc atoms to generate a 2-fold interpenetrated framework filled with coordinated dimethylformamide and ethanol molecules (Figure 1).<sup>13,15</sup> The Zn<sub>2</sub> clusters and V-shaped building blocks self-assemble to form a porous framework with two different cavities that contain a molecular square composed of two tetrazinc clusters and two molecules of 2,20-bis(4-carboxyphenyl)hexafluoropropane (CPHFP). The framework also contains a helical structure composed of tetrazinc clusters and two molecules of CPHFP with a void space of 133 Å<sup>3</sup> running along the *b*-axis after removing one of the ethanol molecules. Crystal structure analysis suggests the tubular cavities with 4.67 Å × 4.78 Å dimensions connected with a pore opening diameter of 5.53 Å. The framework topology may be reduced by viewing the zinc cluster as a hexacoordinate antiprism in which four zinc atoms are connected to six carboxylate groups of CPHFP. Figure 1 illustrates one octahedron bound to six organic building blocks,

Received: March 1, 2012

Published: May 16, 2012

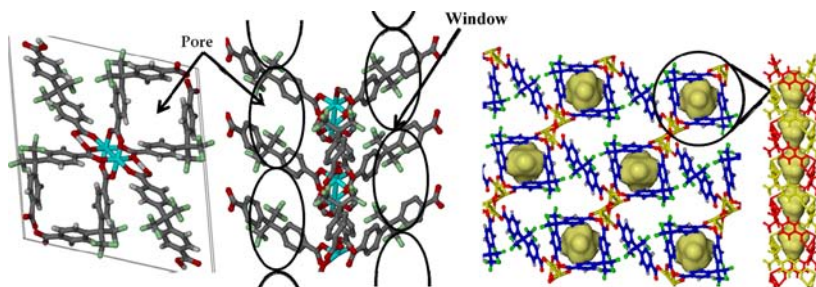


**Figure 1.** Crystal structure of FMOFZn (right) and FMOF-Cu (left). Note the 1D open channels connected through bottleneck windows in FMOFCu.

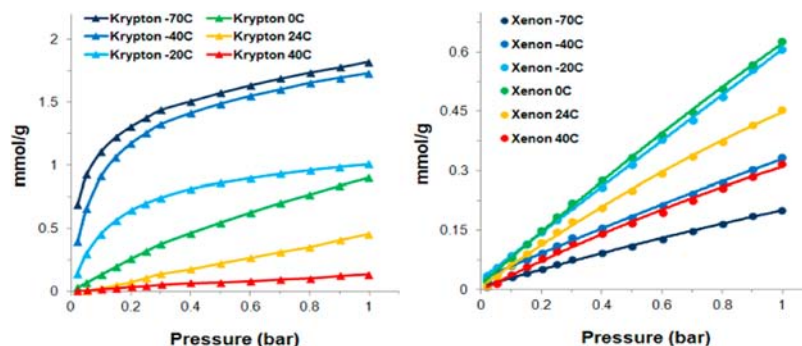


**Figure 2.** Xe and Kr sorption isotherms for FMOFCu at various temperatures. Note the decrease in Xe uptake below 0 °C at all pressures.

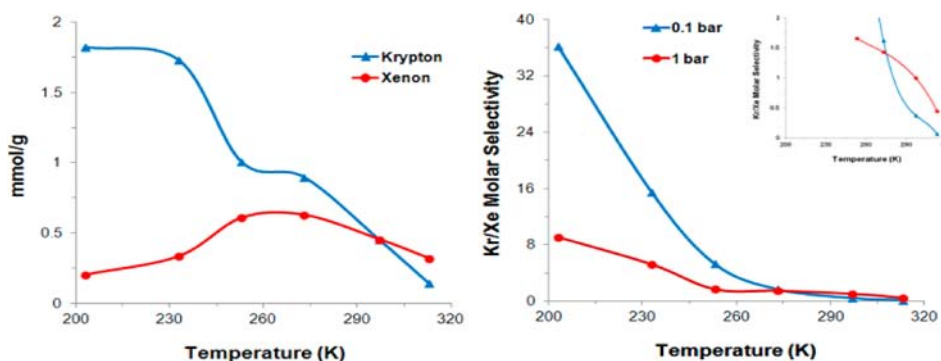


**Figure 3.** Kr and Xe adsorption as a function of temperature at 1 bar (left). The Kr/Xe selectivity in FMOFCu is inverted at 0 °C. Estimated Kr/Xe molar selectivities from pure gas isotherms as a function of temperature at 0.1 and 1 bar (Right) (Inset shows a 270–313 K temperature range).

and the repetition of the same unit in three dimensions results in a framework that is complicated by the presence of two identical, interpenetrating strands.<sup>13,14,15b</sup> In contrast, FMOF-Cu shows a 3D interpenetrating framework containing ordered 1D channels built on Cu<sub>2</sub> paddle wheels (Figure 1). Each Cu center has a square-pyramidal coordination environment with two Cu-atoms sharing four carboxylate groups of the four CPHFP ligand, which are located in the equatorial plane, to form a paddle wheel with a Cu–Cu interatomic distance of 2.645 Å. The 3D network is generated by the connection of adjacent 2D layers via monodentate carboxylate groups of CPHFP ligands that bind to the apical position of the metal centers. An important feature of this porous material is that these tubular cavities with 5.1 Å × 5.1 Å dimensions are connected through small (bottleneck) windows (3.5 Å × 3.2 Å) (Figure 1).<sup>14</sup> Although FMOFCu cages have a larger size than the kinetic diameters of Xe and Kr (3.96 and 3.60 Å), we selected this material because the connecting windows have dimensions practically similar (based on atom to atom distances) to the kinetic diameter of Kr (3.60 Å) and are

smaller than the corresponding Xe diameter (3.96 Å). Therefore, Xe diffusion inside the cavities will be restricted; hence, FMOFCu may be potentially selective toward Kr capture *via* molecular sieving compared to FMOFZn where connecting windows are much larger than kinetic diameter of Xe and Kr.

Thermogravimetric analysis coupled with mass spectrometry (TG-MS) was performed on FMOFZn and FMOFCu. The TG-MS shows 20% and 28% of weight loss between rt and 220 °C corresponding to the loss of DMF and ethanol molecules or water molecules, respectively (Figure S1). The porosity was confirmed by N<sub>2</sub> adsorption at 77 K. FMOFZn showed a surface area of 370 m<sup>2</sup> g<sup>-1</sup> while FMOF-Cu showed 58 m<sup>2</sup> g<sup>-1</sup> (Figures S2 and S3). Variable-temperature and pressure powder X-ray diffraction (pXRD) on FMOFZn suggests considerable change in the powder pattern between 120 and 140 °C (Figure S4).<sup>6,13</sup> This behavior has been ascribed to the framework reorganization upon solvent removal. Similarly, there was no detectable change in pXRD after solvent removal was observed for FMOFCu, indicating structural stability (Figure S5).

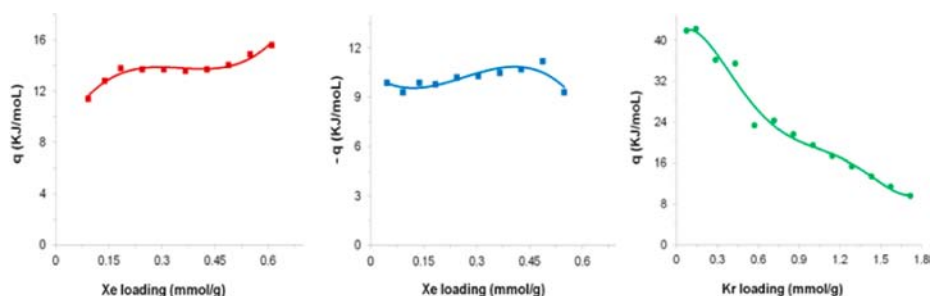


**Figure 4.** Isosteric enthalpies of adsorption as a function of Xe loading in **FMOFCu** (left and middle) showing two different trends below (endothermic heats of adsorption) and above (exothermic heats of adsorption) 0 °C. Similarly, isosteric heats of adsorption as a function of Kr loading on **FMOFZn** (right).

Pure Kr and Xe adsorption/desorption experiments were performed at various temperatures on **FMOFCu** and **FMOFZn**. Figure 2 shows the adsorption isotherms for Kr and Xe at six different temperatures. The isotherms at each temperature show a gradual gain in uptake with pressure with no saturation at 1 bar. Similar trends were observed for **FMOFZn** (Figure S6). The adsorption values increase for both Kr and Xe as the temperature decreases, which is the expected behavior for most MOFs. Desorption profiles on **FMOFCu** and **FMOFZn** indicate no obvious hysteresis for either Xe or Kr (Figures S7). A significant result is the faster increase in Kr uptake as the temperature is decreased as compared to Xe. Figure 2 also shows that, at rt, the capacity for Kr is comparable to that observed for Xe at all pressures and the selectivity of **FMOFCu** toward these gases seems to revert below rt. This was not observed in **FMOFZn** (Figure S7). The inversion in Kr and Xe selectivity in **FMOFCu** was clearly observed in Figure 3 (left) where a plot of the sorption of Kr and Xe as a function of temperature is shown at 1 bar. The figure shows a rapid increase in uptake for both gases; however, this increase (as described above) is at a faster rate for Kr. Furthermore, the adsorption of Xe below 0 °C begin to decrease and reaches sorption values lower than that of 40 °C. In addition the Xe and Kr adsorption isotherms obtained at −40 and 40 °C (Figure S8) further demonstrate the inversion in Kr and Xe selectivity. The Kr and Xe molar selectivity as a function of temperature (270–313 K) was estimated using the pure gases isotherms (Figure 3). It can be clearly seen that the selectivity reverts below rt and increases nearly exponentially with decreasing temperatures at 0.1 bar. At this pressure and 203 K, the material shows an estimated Kr/Xe molar selectivity of 36 as compared to Kr/Xe = 0.45 at 40 °C.

This behavior is of significant magnitude because it shows for the first time that a MOF reverses its selectivity toward Xe and Kr by simply decreasing the temperature. This phenomenon can be ascribed to two different processes that may be occurring simultaneously. One has to do with a temperature-dependent gating effect, which has been reported by Zhou et al.<sup>16</sup> At low enough temperatures, the window space becomes inaccessible by Xe molecules due to the lower kinetic energy of the adsorbate molecule, which cannot overcome potential barriers at the aperture of the pores that can otherwise accommodate them. These potential barriers are related to the thermal vibration of the flexible windows functioning as gates in **FMOFCu**. In other words, the decreasing flexibility (*via* decreasing sorbent temperature) of the windows in the porous material seems to compromise the diffusion of the larger Xe molecules inside the channels and the kinetic effect (adsorbate

diffusivity) outperforms the thermodynamic effect. On the other hand, the adsorption of Kr (lighter and smaller molecule) is dominated by the thermodynamic effect; i.e., the sorbent/sorbate interaction is stronger as the temperature decreases. This can be seen in Figure 3 (left) where plotting Xe and Kr adsorption of **FMOFCu** shows a distinct molecular sieving effect at <0 °C, where the smaller gas Kr shows larger adsorption values than the larger gas Xe. Another possibility is related to the adsorption taking place above and below a critical temperature. Although in bulk Xe behaves as a gas at the pressures and temperatures studied, the phase behavior can be different in a confined nanoenvironment.<sup>17</sup> Therefore, below a critical temperature condensation at the small pore windows in **FMOFCu** can, in principle, occur. This will then prevent subsequent Xe molecules from penetrating the pore channels resulting in low Xe adsorption. These two processes should not take place in **FMOFZn** since the cavities and windows are large enough to accommodate both gases. As a result **FMOFCu** is potentially selective toward Kr over Xe at relatively moderate temperatures, which is of significant industrial importance. To obtain further information about the actual Kr/Xe selectivities on **FMOFCu**, breakthrough experiments at two different temperatures (25 and 5 °C; see Supporting Information, Figure S9) were performed. The results for a Xe/Kr 1:1 mixture where the Kr/Xe selectivity of **FMOFCu** increases as the temperature decreases (Kr/Xe = 0.6 at rt and Kr/Xe = 0.9 at 5 °C), which is consistent from the selectivities calculated using pure gas isotherms. This indicates that, at <0 °C, Kr/Xe selectivities greater than 1 may be achieved.

Variable temperature and pressure powder X-ray diffraction (pXRD) experiments were conducted to study possible structural transformations of **FMOFCu** (Supporting Information, Figure S10). No obvious changes in the pXRD pattern were observed due to the loading of Xe or Kr. Nonetheless, with the purpose of learning about the thermal energy involved in the sorption of these two gases in **FMOFCu** and to correlate the heats of adsorption with the observed Kr and Xe selectivity-versus-temperature trends, we calculated the isosteric heats of adsorption using the Clausius–Clapeyron equation. Figure 4 shows the enthalpies of adsorption obtained for Kr as a function of gas loading for **FMOFCu**. Krypton shows large (exothermic) enthalpy values at low Kr loadings, and these energy values continuously decrease as Kr loading increases in **FMOFCu**. This behavior is consistent with a porous material with open sites that show high Kr affinity, and as these sites become saturated, Kr fills the center of the cavities in the framework with correspondingly lower enthalpies of adsorption. However, we observed a very interesting behavior for Xe

enthalpies of adsorption. When plotting  $\ln P$  as a function of  $1/T$ , we noticed for all Xe loadings a parabolic behavior instead of the typical straight line. Therefore, we plotted heats of adsorption as a function of Xe loading in two temperature ranges: 203–273 K and 273–313 K (Figure 4, middle and right plot). At  $>0$  °C, the enthalpies of adsorption (exothermic values) are fairly constant with Xe loading and lower than Kr enthalpies of adsorption, particularly at low Xe loadings. This result seems rather unexpected because Xe is a highly polarizable molecule that would interact with the open metal centers in the FMOFCu cavities similarly to Kr. However, the size of the Xe molecule is slightly larger than the dimensions of the connecting windows ( $3.5 \text{ \AA} \times 3.2 \text{ \AA}$  based on atom to atom distances) and this would affect the diffusion of Xe inside the framework cavities. This was particularly evident for the isosteric heats of adsorption calculated at  $<0$  °C (Figure 4, middle). The enthalpy values as a function of Xe loading were constant but positive independently of Xe loading, showing endothermic behavior during Xe sorption at low temperatures. These results correlate very well with the observed decrease of Xe capacity on FMOFCu at  $<0$  °C. Although it was not possible to obtain the unit cell parameters after evacuation, these results are of special significance because it seems evident that the diffusion of this larger molecule is compromised as the temperature of the porous material decreases.

As described earlier, this behavior may have to do with either a temperature gating mechanism or condensation of Xe below the critical temperature; the decrease in flexibility of the connecting windows in the FMOFCu creating a potential barrier for Xe molecules at the aperture of the pores and the Xe condensation at the pore windows (gate). Krypton, a smaller molecule with a size similar to that of the FMOFCu cavity connecting windows, seems to show no diffusion-restricted adsorption. Therefore, the difference in kinetic diameters between these two, otherwise chemically similar, gases and the dimensions of the framework connecting window in FMOFCu seems to be the main reason why the observed estimated Kr/Xe selectivities increase dramatically as the experimental temperatures are decreased.

In summary, we reported the Xe and Kr sorption properties of two partially fluorinated MOFs and demonstrated for the first time that a MOF material can selectively capture and separate Kr from Kr/Xe mixtures at moderate temperature.

## ■ ASSOCIATED CONTENT

### 📄 Supporting Information

TGMS, pXRD, BET, and breakthrough experiments are described in detail in the Supporting Information. This material is available free of charge via the Internet at <http://pubs.acs.org>.

## ■ AUTHOR INFORMATION

### Corresponding Author

praveen.thallapally@pnnl.gov

### Notes

The authors declare no competing financial interest.

## ■ ACKNOWLEDGMENTS

P.K.T. and D.M.S. would like to acknowledge the U.S. DOE Office of Nuclear Energy for financial support.

## ■ REFERENCES

- (1) Izumi, J. In *Handbook of Zeolite Science and Technology*; Auerbach, S. M., Carrado, K. A., Dutta, P. K., Eds.; CRC Press: New York, 2003.
- (2) Jameson, C. J.; Jameson, A. K.; Lim, H. M. *J. Chem. Phys.* **1997**, *107*, 4364.
- (3) (a) Li, H.; Eddaoudi, M.; O'Keeffe, M.; Yaghi, O. M. *Nature* **1999**, *402*, 276. (b) Eddaoudi, M.; Kim, J.; Rosi, N. L.; Vodak, D. T.; Wachter, J.; O'Keeffe, M.; Yaghi, O. M. *Science* **2002**, *295*, 469. (c) Uemura, T.; Yanai, N.; Kitagawa, S. *Chem. Soc. Rev.* **2009**, *38*, 1228.
- (4) (a) Banerjee, R.; Phan, A.; Wang, B.; Knobler, C.; Furukawa, H.; O'Keeffe, M.; Yaghi, O. M. *Science* **2008**, *319*, 939. (b) An, J.; Farha, O. K.; Hupp, J. T.; Pohl, E.; Yeh, J.; Rosi, N. L. *Nat. Commun.* **2012**, DOI: doi: 10.1038/ncomms1618.
- (5) (a) Ko, N.; Go, Y. B.; Aratani, N.; Choi, S. B.; Choi, E.; Yazaydin, A. O.; Snurr, R. Q.; O'Keeffe, M.; Kim, J.; Yaghi, O. M. *Science* **2010**, *329*, 424. (b) Farha, O. K.; Yazaydin, O.; Eryazici, I.; Malliakas, C.; Hauser, B.; Kanatzidis, M. G.; Nguyen, S. T.; Snurr, R. Q.; Hupp, J. T. *Nat. Chem.* **2010**, *2*, 944.
- (6) (a) Férey, G. *Chem. Soc. Rev.* **2008**, *37*, 191. (b) Thallapally, P. K.; Tian, J.; Kishan, M. R.; Fernandez, C. A.; Dalgarno, S. J.; McGrail, P. B.; Warren, J. E.; Atwood, J. L. *J. Am. Chem. Soc.* **2008**, *130*, 16842.
- (7) Some recent reviews include: (a) O'Keeffe, M.; Yaghi, O. M. *Chem. Rev.* **2012**, *112*, 675. (c) Sumida, K.; Rogow, D. L.; Mason, J. A.; McDonald, T. M.; Bloch, E. D.; Herm, Z. R.; Bae, T. H.; Long, J. R. *Chem. Rev.* **2012**, *112*, 724. (d) Li, J.-R.; Sculley, J.; Zhou, H.-C. *Chem. Rev.* **2012**, *112*, 869. (e) Kreno, L. E.; Leong, K.; Farha, O. K.; Allendorf, M.; Van Duyn, R. P.; Hupp, J. T. *Chem. Rev.* **2012**, *112*, 1105. (f) Bae, Y. S.; Snurr, R. Q. *Angew. Chem., Int. Ed.* **2011**, *50*, 2. (g) Wang, C.; Zhang, T.; Lin, W. *Chem. Rev.* **2012**, *112*, 1084. (i) Perry, J. J.; Perman, J. A.; Zaworotko, M. J. *Chem. Soc. Rev.* **2009**, *38*, 1400. (j) Liu, J.; Thallapally, P. K.; McGrail, B. P.; Brown, D. R.; Liu, J. *Chem. Soc. Rev.* **2012**, *41*, 2308. (k) Ma, S.; Meng, L. *Pure Appl. Chem.* **2011**, *83*, 167. (l) Chen, B.; Xiang, S.; Qian, G. *Acc. Chem. Res.* **2010**, *43*, 1115. (m) Chapman, K. W.; Sava, D. F.; Halder, G. J.; Chupas, P. J.; Nenoff, T. N. *J. Am. Chem. Soc.* **2011**, *133*, 18583.
- (8) (a) Bae, Y.-S.; Hauser, B.; Snurr, R. Q.; Hupp, J. T. *Microporous Mesoporous Mater.* **2011**, *141*, 231. (b) Zheng, B.; Bai, J.; Duan, J.; Wojtas, L.; Zaworotko, M. J. *J. Am. Chem. Soc.* **2011**, *133*, 748. (c) Lee, C. Y.; Bae, Y.-S.; Jeong, N. C.; Farha, O. K.; Sarjeant, A. A.; Stern, C. L.; Nickias, P.; Snurr, R. Q.; Hupp, J. T.; Nguyen, S. T. *J. Am. Chem. Soc.* **2011**, *133*, 5228.
- (9) Mueller, U.; Schubert, M.; Teich, F.; Puetter, H.; Schierle-Arndt, K.; Pastre, J. *J. Mater. Chem.* **2006**, *16*, 626.
- (10) Thallapally, P. K.; Grate, J. W.; Motkuri, R. K. *Chem. Commun.* **2012**, *48*, 347.
- (11) (a) Ryan, P.; Farha, O. K.; Broadbelt, L. J.; Snurr, R. Q. *AIChE J.* **2011**, *57*, 1759. (b) Sikora, B. J.; Wilmer, C. E.; Greefield, M. L.; Snurr, R. Q. *Chem. Sci.* **2012**, DOI: doi: 10.1039/C2SC01097F.
- (12) Greathouse, J. A.; Kinnibrugh, T. L.; Allendorf, M. D. *Ind. Eng. Chem. Res.* **2009**, *48*, 3425.
- (13) Fernandez, C. A.; Thallapally, P. K.; Motkuri, R. K.; Nune, S. K.; Sumrak, J. C.; Tian, J.; Liu, J. *Cryst. Growth Des.* **2010**, *10*, 1037.
- (14) Pan, L.; Sander, M. B.; Huang, X. Y.; Li, J.; Smith, M.; Bittner, E.; Bockrath, B.; Johnson, J. K. *J. Am. Chem. Soc.* **2004**, *126*, 1308.
- (15) (a) Zou, R.-Q.; Zhong, R.-Q.; Du, M.; Kiyobayashi, T.; Xu, Q. *Chem. Commun.* **2007**, 2467. (b) Monge, A.; Snejko, N.; Gutiérrez-Puebla, E.; Medina, M.; Cascales, C.; Ruiz-Valero, C.; Iglesias, M.; Gómez-Lor, B. *Chem. Commun.* **2005**, 1291. (c) Liu, Z.; Stern, C.-L.; Lambert, J. B. *Organometallics* **2009**, *28*, 84.
- (16) (a) Ma, S.; Sun, D.; Wang, Z.-S.; Zhou, H.-C. *Angew. Chem., Int. Ed.* **2007**, *46*, 2458. (b) Zhou, D.; Yuan, D.; Krishna, R.; Van Baten, J. M.; Zhou, H.-C. *Chem. Comm* **2010**, *46*, 7352.
- (17) Walton, K. S.; Millward, A. R.; Dubbeldam, D.; Frost, H.; Low, J. J.; Yaghi, O. M.; Snurr, R. Q. *J. Am. Chem. Soc.* **2008**, *130*, 406.